HOMODYNING BELL'S INEQUALITY

G. M. D'Ariano[1,2], L. Maccone[2], M. F. Sacchi[2] and A. Garuccio[3]

[1]Department of Electrical and Computer Engineering,
Northwestern University, Evanston, IL 60208

[2]Theoretical Quantum Optics Group
Università degli Studi di Pavia and INFM — Unità di Pavia
via A. Bassi 6, I-27100 PAVIA, Italy

[3]Dipartimento Interateneo di Fisica
Università degli Studi di Bari and
INFN, Sezione D, I-70126 BARI, Italy

Abstract

We propose to test Bell's inequality through homodyne tomography. The experimental apparatus is mainly composed of a nondegenerate optical parametric amplifier and four photodiodes. The experimental data are gathered through a self–homodyne scheme and are processed by quantum tomography. Our procedure does not introduce supplementary hypotheses (fair sampling assumption), since we do not need to collect auxiliary data to normalize probabilities. Moreover in the proposed experiment, the minimum value of detector quantum efficiency η is virtually reduced down to $\eta = .5$ (in practice to $\eta \sim 65 \div 70\%$). The feasibility of the experiment is shown by some numerical results based on Monte–Carlo simulations.

INTRODUCTION

In a typical experiment to test Bell's inequality that involve optical radiation the source emits a pair of correlated photons and two detectors separately check the presence of the two photons after polarizing filters at angles α and β, respectively. Alternatively, one can use four photodetectors with polarizing beam splitters in front, with the advantage of checking through coincidence counts that photons come in pairs. Let $p_{\alpha,\beta}$ be the joint probability of finding one photon at each detector with polarization angle α and β, respectively. In terms of the correlation function

$$C(\alpha, \beta) = \; p_{\alpha,\beta} + p_{\bar{\alpha},\bar{\beta}} - p_{\bar{\alpha},\beta} - p_{\alpha,\bar{\beta}} \;, \tag{1}$$

Bell's inequality [1] writes as follows

$$B(\alpha, \beta, \alpha', \beta') \doteq |C(\alpha, \beta) - C(\alpha, \beta')| + |C(\alpha', \beta') + C(\alpha', \beta)| \leq 2 \;, \tag{2}$$

$\bar{\alpha}$ and $\bar{\beta}$ denoting the polarization angles orthogonal to α and β respectively. In this paper we propose a new kind of test for Bell's inequality based on quantum homodyne tomography [2, 3] (for a review see Ref. 4). In our setup the photodetectors are replaced by homodyne detectors, which allows measuring the joint probabilities $p_{\alpha,\beta}$ through the tomographic technique. The main advantage of the tomographic test is that linear photodiodes with available quantum efficiency η higher than 90% [5] can be used. On the other hand, the method works effectively even with η as low as 70%, without the need of a "fair sampling" assumption,[6, 7] since all data are collected in a single experimental run. In the present case the customary homodyne technique would need many additional beam splitters and local oscillators (LO) that are coherent each other. As we will show, the setup is greatly simplified by using the recent self-homodyne technique.[8] Another advantage of self-homodyning is the more efficient signal-LO mode-matching, with improved overall quantum efficiency.
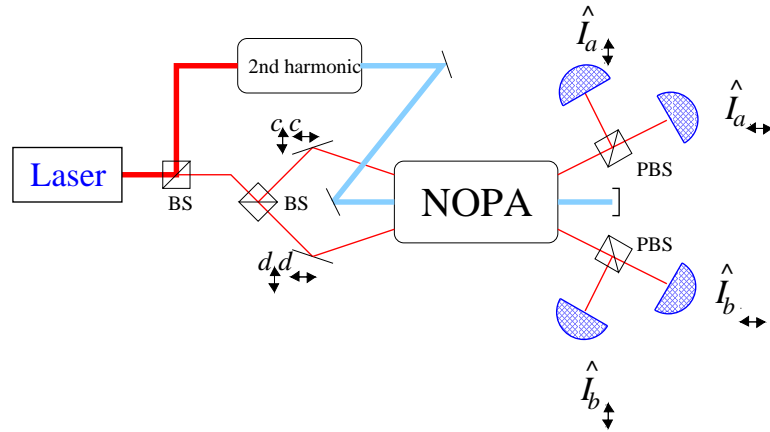

Figure 1. Self-homodyne scheme for the tomographic test of Bell's inequality. PBS and BS denote 'polarizing beam splitter' and 'conventional beam splitter' respectively. Input radiation modes $a_\updownarrow$, $b_\leftrightarrow$, $a_\leftrightarrow$ and $b_\updownarrow$ are in the vacuum state, while modes $c_\updownarrow$, $c_\leftrightarrow$, $d_\updownarrow$, $d_\leftrightarrow$ (at laser frequency ω_0) are in a coherent state. At the output of the nondegenerate parametric amplifier (NOPA) the four photocurrents $\hat{I}$ at radiofrequency Ω are detected, yielding the value of the quadratures of the field modes $a_\updownarrow$, $b_\leftrightarrow$, $a_\leftrightarrow$ and $b_\updownarrow$. The outcome quadratures are then used to reconstruct the probabilities of interest through quantum tomography.

THE EXPERIMENTAL SET-UP

The apparatus for generating the correlated beams is a nonlinear crystal, cut for Type-II phase–matching, acting as a nondegenerate optical parametric amplifier (NOPA). The NOPA is injected with excited coherent states (see Fig. 1) in modes $c_\leftrightarrow, c_\updownarrow, d_\leftrightarrow, d_\updownarrow$ all with equal intensities and at the same frequency ω_0, c and d denoting mode operators for the two different wave-vector directions, and $\updownarrow$ and $\leftrightarrow$ representing vertical and horizontal polarization, respectively. The NOPA is pumped at the second harmonic $2\omega_0$. At the output of the amplifier four photodetectors separately measure the intensities $\hat{I}_{a_\updownarrow}$, $\hat{I}_{b_\leftrightarrow}$, $\hat{I}_{a_\leftrightarrow}$, $\hat{I}_{b_\updownarrow}$ of the mutual orthogonal polarization components of the fields propagating at different wave vectors. The output photocurrent is narrow-band filtered at radiofrequency $\Omega \ll \omega_0$. In the process of direct detection, the central modes $c_{\updownarrow,\leftrightarrow}$ and $d_{\updownarrow,\leftrightarrow}$ beat with $\omega_0 \pm \Omega$ sidebands, thus playing the role of the LO in homodyne detectors. The four photocurrents $\hat{I}_{a_\updownarrow}$, $\hat{I}_{b_\leftrightarrow}$, $\hat{I}_{a_\leftrightarrow}$, $\hat{I}_{b_\updownarrow}$ yield the value of the

quadratures of the four modes [8]

$$s_\pi = \frac{1}{\sqrt{2}}\left(s_\pi(+) + s_\pi(-)\right), \qquad s = \{a, b\} \qquad \pi = \{\leftrightarrow, \updownarrow\}, \tag{3}$$

where $a_\pi(\pm)$ and $b_\pi(\pm)$ denote the sideband modes at frequency $\omega_0 \pm \Omega$, which are in the vacuum state at the input of the NOPA. The quadrature is defined by the operator $\hat{x}_\phi \doteq \frac{1}{2}(ae^{-i\phi} + a^\dagger e^{i\phi})$, where ϕ is the relative phase between the signal and the LO. The value of the quadratures is used as input data for the tomographic measurement of the correlation function $C(\alpha, \beta)$. The direction of polarizers (α, β) in the experimental setup does not need to be varied over different trials, because, as we will show in the following, such direction can be changed tomographically.

Under condition of phase-matching and in the parametric approximation, the spontaneous down-conversion at the NOPA is described in terms of the field modes in Eq. (3) by the unitary evolution operator

$$\hat{U}(\xi) = \exp\left[\xi\left(a_\updownarrow^\dagger b_\leftrightarrow^\dagger + e^{i\varphi}a_\leftrightarrow^\dagger b_\updownarrow^\dagger\right) - \text{h. c.}\right], \tag{4}$$

where $\xi = \chi\gamma L/c$ is a rescaled interaction time evaluated by the nonlinear susceptibility χ of the medium, the crystal length L, the pump amplitude γ and the speed c of light in the medium, whereas φ represents the relative phase between the orthogonal polarization components of the pump field. Correspondingly, the state at the output of the NOPA writes as follows

$$|\psi\rangle = (1 - |\Lambda|^2)\sum_{n=0}^{\infty}\sum_{m=0}^{\infty}\Lambda^{n+m}e^{i\varphi m}|n, n, m, m\rangle \equiv |\psi_{1,2}\rangle \otimes |\psi_{3,4}\rangle, \tag{5}$$

where $\Lambda = \xi \tanh|\xi|/|\xi|$ and $|i, l, m, n\rangle$ denotes the common eigenvector of the number operators of modes $a_\updownarrow$, $b_\leftrightarrow$, $a_\leftrightarrow$, $b_\updownarrow$, with eigenvalues i, l, m and n, respectively. The average photon number *per* mode is given by $N = |\Lambda|^2/(1 - |\Lambda|^2)$. The four-mode state vector in Eq. (5) factorizes into a couple of twin beams $|\psi_{1,2}\rangle$ and $|\psi_{3,4}\rangle$, each one entangling a couple of spatially divergent modes ($a_\updownarrow$, $b_\leftrightarrow$ and $a_\leftrightarrow$, $b_\updownarrow$, respectively).

HOMODYNING BELL'S INEQUALITY

The conventional experiments that involve a two-photon polarization-entangled state generated by spontaneous down-conversion, consider the four-mode entangled state which can be obtained by keeping only the first-order terms of the sums in Eq. (5), and by ignoring the vacuum component, as usually only intensity correlations are measured. Here, on the contrary, we measure the joint probabilities on the state (5) to test Bell's inequality through homodyne tomography, which yields the value of $B(\alpha, \beta, \alpha', \beta')$ in Eq. (2). The tomographic technique is a kind of universal detector, which can measure any observable $\hat{O}$ of the field, by averaging a suitable "pattern" function $\mathcal{R}[\hat{O}](x, \phi)$ over homodyne data x at random phase ϕ. The "pattern" function is obtained through the trace relation [9]

$$\mathcal{R}[\hat{O}](x, \phi) = \text{Tr}\left[\hat{O}K_\eta(x - \hat{x}_\phi)\right], \tag{6}$$

where $K_\eta(x)$ is a distribution given in Ref. 10. For factorized many-mode operators $\hat{O} = \hat{O}_1 \otimes \hat{O}_2 \otimes ... \otimes \hat{O}_n$ the pattern function is just the product of those corresponding to each single-mode operator $\hat{O}_1, ..., \hat{O}_n$ labelled by variables $(x_1, \phi_1), ..., (x_n, \phi_n)$. By linearity the pattern function is extended to generic many-mode operators.

Now we consider the observables that are involved in testing Bell's inequality (2). Let us denote by $p_{\alpha,\beta}(i,l,m,n)$ the probability of having i,l,m,n photons in modes $a_\updownarrow, b_\leftrightarrow, a_\leftrightarrow, b_\updownarrow$ for the "rotated" state

$$|\psi\rangle_{\alpha,\beta} \equiv \hat{U}_{1,3}(\alpha)\hat{U}_{2,4}(\beta)|\psi\rangle \ , \tag{7}$$

$\hat{U}_{1,3}(\alpha)$ and $\hat{U}_{2,4}(\beta)$ being the unitary operators

$$\hat{U}_{1,3}(\alpha) = \exp\left[\alpha\left(a_\updownarrow^\dagger a_\leftrightarrow - a_\updownarrow a_\leftrightarrow^\dagger\right)\right] \ , \tag{8}$$

$$\hat{U}_{2,4}(\beta) = \exp\left[\beta\left(b_\updownarrow^\dagger b_\leftrightarrow - b_\updownarrow b_\leftrightarrow^\dagger\right)\right] \ . \tag{9}$$

The probabilities in Eq. (1) can be written as $p_{\alpha,\beta} = p_{\alpha,\beta}(1,1)$, $p_{\bar{\alpha},\bar{\beta}} = p_{\alpha,\beta}(0,0)$, $p_{\bar{\alpha},\beta} = p_{\alpha,\beta}(0,1)$, and $p_{\alpha,\bar{\beta}} = p_{\alpha,\beta}(1,0)$, with

$$p_{\alpha,\beta}(n,m) = \frac{p_{\alpha,\beta}(n,1-m,1-n,m)}{P(1,1)} \ , \qquad \{n,m=0,1\} \ . \tag{10}$$

The denominator $P(1,1)$ in Eq. (10) represents the absolute probability of having at the output of the NOPA one photon in modes $a_\updownarrow, a_\leftrightarrow$ and one photon in modes $b_\updownarrow, b_\leftrightarrow$, independently on the polarization, namely

$$P(1,1) = \sum_{n=0,1}\sum_{m=0,1} p_{\alpha,\beta}(n,1-m,1-n,m) \ . \tag{11}$$

In our procedure both the numerator and the denominator of Eq. (10) are measured in only one run, hence we do not need a fair sampling assumption, namely we do not have to collect auxiliary data to normalize probabilities. Moreover, since we can exploit quantum efficiencies as high as $\eta = 90\%$ and the tomographic pattern functions in Eq. (6) already take into account η, we do not need supplementary hypothesis for it.[7]

The observables that correspond to probabilities $p_{\alpha,\beta}(i,l,m,n)$ in Eqs. (10) and (11) are the projectors

$$|i,l,m,n\rangle_{\alpha,\beta}\ _{\alpha,\beta}\langle i,l,m,n| = \hat{U}_{1,3}^\dagger(\alpha)\,\hat{U}_{2,4}^\dagger(\beta)\,|i,l,m,n\rangle\langle i,l,m,n|\,\hat{U}_{2,4}(\beta)\,\hat{U}_{1,3}(\alpha) \ . \tag{12}$$

¿From Eqs. (6) and (10,11,12), one finds that $P(1,1)$ is measured through the following average $\mathcal{AV}$ of homodyne data

$$P(1,1) = \mathcal{AV}\left\{\left(K_1^1 K_0^3 + K_0^1 K_1^3\right)\left(K_1^2 K_0^4 + K_0^2 K_1^4\right)\right\} \ , \tag{13}$$

where K_n^j denotes the diagonal tomographic kernel function for mode j, namely

$$K_n^j \equiv \langle n|K_\eta(x - \hat{x}_{\phi_j})|n\rangle \ . \tag{14}$$

The kernel function for the numerator of Eq. (10) involves both the diagonal terms (14) and the following off-diagonal terms

$$K_+^j \equiv \langle 0|K_\eta(x - \hat{x}_{\phi_j})|1\rangle \ , \qquad K_-^j = (K_+^j)^* \ . \tag{15}$$

Finally, the expression for $C(\alpha,\beta)$ in Eq. (1) is given by

$$C(\alpha,\beta) = \mathcal{AV}\Big\{[\,\cos(2\alpha)\left(K_1^1 K_0^3 - K_0^1 K_1^3\right) + \sin(2\alpha)\left(K_+^1 K_-^3 + K_-^1 K_+^3\right)] \tag{16}$$

$$\times[\,\cos(2\beta)\left(K_0^2 K_1^4 - K_1^2 K_0^4\right) + \sin(2\beta)\left(K_+^2 K_-^4 + K_-^2 K_+^4\right)]\Big\}/P(1,1) \ .$$

The statistical error for $B(\alpha,\beta,\alpha',\beta')$ in Eq. (2) can be obtained from the variance calculated upon dividing the set of data into large statistical blocks. However, $C(\alpha,\beta)$—and thus $B(\alpha,\beta,\alpha',\beta')$— are non linear averages (they are ratios of averages). Hence, since the nonlinearity of B introduces a systematical error which is vanishingly small for increasingly larger sets of data, the estimated mean value of B is obtained from the full set of data, instead of averaging the mean value of the blocks.

SOME NUMERICAL RESULTS

We now present some numerical results obtained from Monte–Carlo simulations of the proposed experiment. For the simulation we use the theoretical homodyne probability pertaining to the state $|\psi\rangle$ in Eq. (5).
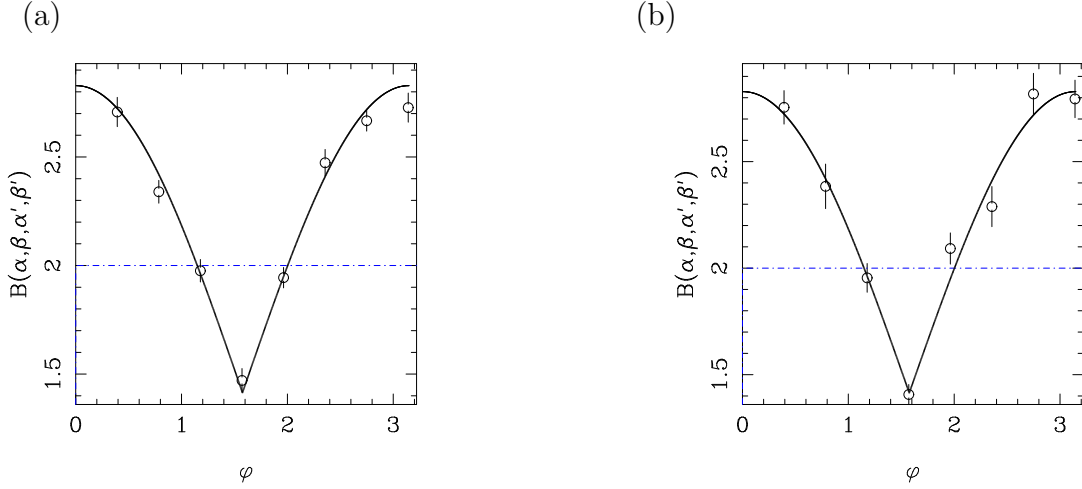
(a) (b)

Figure 2. Plot of $B(\alpha, \beta, \alpha', \beta')$ *vs* the phase φ in the state of Eq. (5) with $N = 0.5$ average photon number *per* mode. The dot-dashed line and the full line represent the classical bound and the quantum theoretical value for B, respectively. The parameters of the simulation are: $\alpha = 0$; $\beta = \frac{3}{8}\pi$; $\alpha' = \frac{\pi}{4}$; $\beta' = \frac{\pi}{8}$. For (a) The quantum efficiency and the number of simulated homodyne data are $\eta = 85\%$ and $n = 10^7$ in (a), and $\eta = 75\%$ and $n = 10^8$ in (b).

In Fig. 2 we present the simulation results for B in Eq. (2) *vs* the phase φ in the state of Eq. (5). The full line represents the value of B evaluated through the quantum theoretical value $C(\alpha, \beta)$ given by

$$C(\alpha, \beta) = \cos\varphi \sin 2\alpha \sin 2\beta - \cos 2\alpha \cos 2\beta . \qquad (17)$$

Quantum efficiency $\eta = 85\%$ has been used in Fig. 2(a), nonetheless notice that for $\varphi = \pi$ (corresponding to a maximum violation with respect to the classical bound 2), the obtained value is over 10 σ distant from the bound. By increasing the number of homodyne data, it is possible to obtain good results also for lower quantum efficiency [see Fig. 2(b), wherein $\eta = 75\%$]. By increasing the number of data to 8×10^8, the value of $B(0, \frac{3}{8}\pi, \frac{\pi}{4}, \frac{\pi}{8}) = 2.834 \pm 0.268$ has been obtained for $\varphi = \pi$, $N = 0.5$ average photon number *per* mode and η as low as 65%. This result is to be compared with the quantum theoretical value of $2\sqrt{2}$. Fig. 3 shows the results of B *vs* different values of the mean photon number *per* mode N for the state in Eq. (5). Notice that the statistical errors are nearly independent on N.

For an order of magnitude of the data acquisition rate in a real experiment, one can consider that in a typical setup with a NOPA pumped by a 2nd harmonic of a Q-switched mode-locked Nd:YAG the pulse repetition rate is 80 MHz, with a 7 ps pulse duration, the effective number of data depending on the speed of the boxcar integrator.

In conclusion we have proposed a test of Bell's inequality, based on self–homodyne tomography. The rather simple experimental apparatus is mainly composed of a NOPA crystal and four photodiodes. The experimental data are collected through a self–homodyne scheme and processed by quantum tomography.
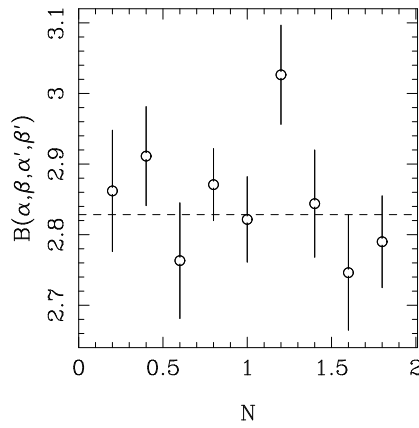
Figure 3. Plot of $B(\alpha, \beta, \alpha', \beta')$ with $\alpha = 0$; $\beta = \frac{3}{8}\pi$; $\alpha' = \frac{\pi}{4}$; $\beta' = \frac{\pi}{8}$ *vs* different values of the mean photon number *per* mode N in the state of Eq. (5). For each simulated experiment, the number of homodyne data is $n = 10^7$ and the quantum efficiency is $\eta = 85\%$. The dotted line represents the quantum theoretical value $2\sqrt{2}$.

No supplementary hypotheses are introduced, a quantum efficiency η as high as 90% is currently available, and, anyway, η as low as 70% is tolerated for $10^7 \div 10^8$ experimental data. We have presented some numerical results based on Monte–Carlo simulations that confirm the feasibility of the experiment, showing violations of Bell's inequality for over $10\,\sigma$ with detector quantum efficiency $\eta = 85\%$.

Acknowledgments

REFERENCES

1. J. S. Bell, Physics **1**, 195 (1965).
2. D. T. Smithey, M. Beck, M. G. Raymer and A. Faridani, Phys. Rev. Lett. **70**, 1244 (1993).
3. G. Breitenbach, S. Schiller and J. Mlynek, Nature **387**, 471 (1997).
4. G. M. D'Ariano, *Measuring quantum states*, in *Quantum Optics and the Spectroscopy of Solids*, ed. by T. Hakioğlu and A.S. Shumovsky, Kluwer Academic Publishers (1997), p. 175.
5. C. Kim and P. Kumar, Phys. Rev. Lett. **73**, 1605 (1994).
6. J. F. Clauser and M. A. Horne, Phys. Rev. D **10**, 256 (1974).
7. L. De Caro and A. Garuccio, Phys. Rev. A **54**, 174 (1996).
8. G. M. D'Ariano, M. Vasilyev and P. Kumar, Phys. Rev. A **58**, 636 (1998).
9. G. M. D'Ariano, in "Quantum Communication, Computing, and Measurement", ed. by O. Hirota, A. S. Holevo and C. M. Caves, Plenum Publishing (New York and London 1997), p. 253.
10. G. M. D'Ariano, U. Leonhardt and H. Paul, Phys. Rev. A **52**, R1801 (1995).